Antheraea proylei J. sericin induces apoptosis in a caspase dependent manner in A549 and HeLa cells and caspase independent manner in PC3 cells

Potsangbam Jolly Devi
Manipur University
Asem Robinson Singh
Manipur University
Lisam Shanjukumar Singh (shanju.lisam@manipuruniv.ac.in)
Manipur University https://orcid.org/0000-0001-5755-2234
Laishram Rupachandra Singh
Manipur University
Sanjenbam Kunjeshwori Devi
Manipur University

Research article

Keywords: Sericin, Antheraea proylei J., silk cocoons, Caspase-3, PARP, MAPK

Posted Date: January 5th, 2021

DOI: https://doi.org/10.21203/rs.3.rs-56346/v2

Abstract

Background

In spite of much progress in understanding the biology of cancer disease, advancement in technology for early diagnosis, the expanding array of anticancer drugs and treatment modalities, the global cancer burden is still significant and increasing. It is estimated that the new cases of cancer in the year 2040 will be 29.4 million per year globally. Sericin, an adhesive protein of silk cocoons has been shown to be a potential protein in various biomedical applications including cancer therapeutics. The present study evaluates the anticancer property of sericin from cocoons *of Antheraea proylei* J. (SAP) against human lung cancer (A549), cervical cancer (HeLa), and prostate cancer (PC3) cell lines. This is the first report of anti-cancer activity of the non-mulberry silkworm *A. proylei* J.

Methods

SAP was prepared from cocoons of *A. proylei* J. by the process of degumming method. The amino acid composition of SAP was determined by HPLC. Cytotoxicity activity was assessed by MTT assay and genotoxicity activity was assessed by comet assay. Cleavage of caspase and PARP proteins and phosphorylation of MAPK pathway members were analysed by Western blotting. Cell cycle analysis was done by flow cytometery.

Results

SAP causes cytotoxicity to A549, HeLa and PC3 cell lines with the IC_{50} values ranging from 3.4-3.9 µg/µl. SAP induces apoptosis in a dose-dependent manner through caspase-3 and p38 and ERK pathways in A549 and HeLa cells respectively whereas in PC3 cells, SAP induces apoptosis independent of caspase through p38 pathway. Moreover, in the case of A549 and HeLa cells SAP induces cell cycle arrest at S phase in a dose dependent manner whereas at G_0 phase in the case PC3 cells.

Conclusion

SAP induces apoptosis in A549, HeLa, and PC3. The difference in the molecular mechanisms of apoptosis induced by SAP in A549 and HeLa and in PC3 may be due to the differences in the genotypes of the cancer cell lines. However, further investigation is warranted. The overall results of the present study envisage the possibility of using SAP as anti-tumorigenic agent.

Introduction

Although we have made much progress in understanding the biology of cancer disease, advancement in technology for early diagnosis, the expanding array of anticancer drugs, and treatment modalities, the global cancer burden remains significant and increasing. It is estimated that new cases of cancer have risen to 18.1 million and deaths due to the disease to 9.6 million in 2018 [1]. Sadly, the estimated new cases of cancer in the year 2040 is 29.4 million per year globally. The increasing trend of cancer burden is

due to several factors, including population growth, aging, as well as the changing prevalence of certain causes of cancer linked to social and economic development particularly in rapidly growing economies [2,3]. In contrast to other world regions, the proportions of cancer deaths in Asia and in Africa (57.3% and 7.3%, respectively) are higher than the proportions of incident cases (48.4% and 5.8%, respectively), because these regions have a higher frequency of certain cancer types associated with poorer prognosis and higher mortality rates, in addition to limited access to timely diagnosis and treatment. The total number of cases of cancer diagnosed in India in between the years 2017 and 2018 is 7,84,821 (an increased by 324%) out of which 4,13,519 are men and 3,71,302 are women [1].

In view of the above facts, there is a need for urgent and serious attention towards finding new anticancer therapeutic drugs to prevent the increasing number of cancer cases in the coming decades in addition to other strategies. One such potential anti-cancer agent is sericin, a silk protein which binds together the silk fibroin fibres to form the cocoon [4]. Silk textile industry targets only the silk fibre obtained after the process of sericin removal, through degumming[5].

Sericin stands as a promising anti-cancer agent which inhibits the growth of cancer cells. The effect of sericin was studied in the colon cancer mice models induced by 1,2-Dimethlhydrazine (DMH). The studies concluded that sericin supplemented diet reduced the formation of colonic aberrant crypt foci [6,7]. Further Zhaorigetu et al., (2001) reported that sericin suppresses the development of colonic tumours by reducing oxidative stress, cell proliferation, and nitric oxide production [8]. The strong antioxidant activity of sericin and its resistance to intestinal proteases prolongs its sustainability in the colon thereby lowering oxidative stress and tumorigenesis in the colon. Yet in another study, sericin was reported to suppress skin tumorigenesis in mice induced by 7,12–dimethybenz (α) anthracene (DMBA) and 12-O-tetradecanoylphorbol 13–acetate (TPA) by reducing oxidative stress, inflammatory responses and endogenous tumour promoter (TNF-α) [9]. It was also observed that sericin from *B. mori* induced apoptosis through caspase pathway and downregulation of Bcl-2 expression in human colorectal cancer cells (SW480) [10]. Kumar & Mandal, (2019)[11] reported anticancer activities of sericin from non-mulberry silkworm *Antheraea assamensis* on MCF-7 and A431 cells through induction of oxidative stress and reduction of mitochondrial membrane potential. Further Zhang et al. (2003)[12], studied the potential of cecropins from *Antheraea pernyi* on inducing apoptosis in human colon adenocarcinoma cell lines. However, detailed studies including molecular mechanisms of inducing apoptosis is poorly understood. The sericin used in most of the previous studies on the prevention and treatment of cancer were obtained from *Bombyx mori or Antheraea sp.* which have been extensively studied.

Depending upon the species of silkworm, the amino acid composition of sericin varies considerably. Sericin from wild silkworms have a higher content of threonine, glutamic acid, cysteine and phenylalanine and a lower content of serine, proline, methionine, glucosamine, galactosamine and histidine [13]. Therefore, sericin from different species of silkworm may have different biological activity and efficacy. The oak tasar silkworm*, A. proylei* J. is reared in several sericulture farms in Manipur and adjoining states and feeds on leaves of oak (*Quercus sp.*) which are naturally grown in the region. The

sericin from *A. proylei* J. silkworm has yet to be explored for its prospective anti-cancer properties and health benefits.

Therefore, the present study aims to evaluate the anticancer property of sericin prepared from cocoons *of Antheraea proylei* J. (SAP) against human lung cancer (A549), cervical cancer (HeLa), and prostate cancer (PC3) cell lines. This is the first study of anti-cancer activity of the non-mulberry silkworm *A. proylei* J. to the best of our knowledge.

Methods:

Extraction of SAP

A. proylei J. cocoons were collected from Uyumpok Tasar Silk Farm, Imphal East, Manipur (24^{o} 57' 2.7396" N, 94^{o} 2' 55.2282" E), India. Five grams of fresh cocoon cut (~ 1 cm^2 pieces) were added to 100 mL distilled water and subjected to heat treatment at 121°C under pressure for 1hr. The resulting suspension was filtered through Whatmann filter paper No.1 and centrifuged at 21,000g for 30 mins. The process was repeated for 2 times with the same cocoon shell sample. The supernatants obtained were pooled and then lyophilized. The lyophilized SAP powder was stored at -20°C until use.

HPLC analysis of predominant amino acids of SAP:

SAP was subjected to acid hydrolysis by dissolving in 6N HCl in boiling water bath for 24 hrs and mixed every hour for proper hydrolysis. It was then centrifuged at 3500 rpm for 15 mins. The supernatant was filtered and neutralized with 1N NaOH. The filtered solution was then diluted to 1:1000 of the volume with milli-Q water and then analyzed for amino acids in HPLC (Agilent 1100 HP), C18, 4.5 X 150, 5µm column using mobile phase A (20 mM sodium acetate + 0.018% triethyalmine, pH to 7.20 ± 0.05) and mobile phase B (20% of 100 mM sodium acetate + 40% methanol and + 40% acetonitrile, pH 7.20 ± 0.05). The flow rate was maintained at 0.5mL/min and the column temperature was kept at 40̊C and detected at 338nm.

Cell lines and culture conditions

Three human cancer cell lines, namely, lung cancer (A549), cervical cancer (HeLa), and prostate cancer (PC3) were obtained from the National Centre for Cell Science (NCCS), Pune, India. All the cell lines were cultured in RPMI 1640 (Gibco, USA) media with 10% FBS (Gibco, USA) and 1% PenStrep (Gibco, USA) and incubated with 5% CO_2 at 37°C.

Cell treatment with SAP

SAP was dissolved in RPMI culture media and centrifuged at 15700g for 30 mins. The supernatant was taken and sterilized through a syringe filter (0.2 µm pore size) for the treatment to the above three cancer cells with different doses (final concentration; 0.17, 0.34, 0.7, 1.4, 2.7, 5.5, and 11µg/µL).

Cell viability assay

Cell viability assay was carried out as per the manufacturer's protocol provided with MTT assay kit, Vybrant MTT assay Kit (Invitrogen Life Technologies). A549, HeLa or PC3 cells were cultured with a density of 1×10^4 cells per well in 100 µL RPMI (without phenol red), 10% FBS and incubated with 5% CO_2 at 37^oC in a 96-well tissue culture plate. Various doses of SAP were treated to the cells in triplicates. After 24 hrs, cell viability was assessed by adding 10µL of 3-(4, 5-dimethylthiazol-2-yl)-2,5-diphenyltetrazolium bromide (MTT) to all the wells followed by incubation at 37^oC for 4 hrs. The formazan crystals formed were dissolved by adding 50µL of DMSO after removal of the culture media and further incubated for 10 mins at room temperature. The numbers of viable cells were then quantified by measuring absorbance at 570 nm. The experiment was conducted in triplicates at least three times.

Comet assay

Comet assay was carried out according to the protocol described by Olive and Banath, 2006 [14]. A549, HeLa, or PC3 cells were treated with various doses of SAP for 24hrs and cells were detached by trypsinization. The number of cells was adjusted at 2×10^4 cells/ml and suspended in PBS. About 400µl of the cell suspension was mixed with 1.2ml of low-melting agarose at 40^oC by gentle pipetting followed by pouring onto agarose pre-coated microscope slides. After proper solidification of the agarose, the slides were submerged in a neutral lysis solution containing 2% SDS, 0.5 mg/ml Proteinase K, 0.5M EDTA and incubated at 37^oC for 16 hrs in the dark. The slides were then washed three times with a neutral rinse buffer followed by electrophoresis at 0.6 V/cm for 25 mins. Slides were then stained with 10µg/ml propidium iodide (PI) and observed under a fluorescence microscope and photographed. The tail lengths of at least 50 comets in each slide were scored for analysis by Leica Application Suite (LAS, GmBH, Germany).

Western blots

A549, HeLa or PC3 cells were seeded in a 60 mm culture dish, grown overnight, and treated with various doses of SAP. The cells were lysed using RIPA buffer and the protein concentration of the cell lysate was estimated using the BCA protein assay kit (Thermo Scientific) and 20 µg of proteins were separated by12% SDS-PAGE. After transferring the separated proteins on PVDF membrane, it was blocked with 5% (w/v) skimmed milk in 1X Tris-buffered saline with 0.1% Tween-20 (TBST) for 1 hr at room temperature. The blocked membranes were then incubated with the primary antibodies (1:1000 dilution) with gentle shaking on a rocker at 4°C overnight. The membrane was probed with antibodies anti-PARP, anti-caspase 3 (both total and cleaved), anti-ERK, anti-p38 or anti-JNK antibodies (both total and phosphorylated) (Cell Signalling, USA). The membranes were then washed with 1X TBST three times for 10 mins each with changes of buffer. After washing the membrane, secondary antibodies conjugated with horseradish peroxidase (HRP) were added at 1:1000 dilutions and kept with gentle shaking for 1hr at room temperature. The membranes were re-blotted with an anti-ß actin antibody to normalize the total protein loaded. The blot was then developed using ECL (GE Amersham) and visualized under BioRad Gel Doc.

MAPK protein inhibition analysis

Cells cultured in 96 well plates were pre-treated with specific inhibitors for p38 (SB203580), SAPK/JNK (SP600125) or ERK (FR180205) proteins 1hr prior to SAP treatment. The treated cells were incubated at 37^{o}C for 24 hrs after which cell survival was quantified by MTT assay. Statistically significance between cells treated with SAP and SAP along with specific inhibitors were determined by unpaired t-test. A p-value of less than 0.05 is considered statistically significant and rescued from apoptosis.

Cell cycle analysis

A549, HeLa, or PC3 cells were cultured in a 6-well culture plate, grown overnight, and treated with various doses of SAP. After 12 hrs, cells were harvested after trypsinization and washed with PBS. The cells were then fixed with ice-cold 70% ethanol added dropwise with regular vortexing to avoid cell clumps and kept at 4°C for 30 mins. The fixed cells were washed twice with PBS by centrifuging at 850 g for 5 mins. Then the cells were treated with 50 µg of RNaseA (100µg/mL) and 200 µL of propidium iodide (PI) (50µg/mL) was added. Cell cycle distribution was analyzed in a FACS flow cytometer (BD Biosciences, USA).

Statistical analysis

Significant variance between groups was performed for all groups with Independent t-test using Graph pad prism 6 Data were expressed as mean±SD. Multiple comparisons among groups were evaluated using Student's t-test. Difference with $p<0.05$(95%CI) were considered statistically significant.

Results:

Amino acid composition of SAP:

The HPLC analysis of SAP for constituent amino acids revealed the presence of aspartic acid, serine, glutamic acid, and histidine in the majority with other essential and non-essential amino acids [Table 1]. The free amino acid composition of SAP from *Antheraea proylei* and comparison with previous reports of sericin from *Bombyx mori* and *Antheraea pernyi* [15,16] is shown in Table 1

SAP induces cytotoxicity to A549, HeLa or PC3 cells in a dose dependent manner.

A549, PC3, or HeLa cells were treated with a various dose of SAP for 24hrs. Morphological changes (rounding up), cell detachment, cell death, and decrease of cell viability were observed after treatment of SAP for 24 hrs [Figure 1(a-f)]. The results showed that SAP induces cytotoxicity in all the cancer cell lines tested in a dose-dependent manner. Further, cells were treated with various dose of SAP (0.17, 0.34, 0.7, 1.4, 2.7, 5.5 and 11µg/µL) for 24 hrs to determine the IC_{50} (half maximal inhibitory concentration) and MTT assay was performed. The results showed that IC_{50} values of SAP for inhibiting the viability of A549, HeLa and PC3 cells were 3.8 µg/µL, 3.9 µg/µL and 3.4 µg/µL respectively [Figure 1(g)] indicating cytotoxic effect.

SAP induces genotoxicity

To ascertain the cytotoxic activity induced by SAP on A549, HeLa and PC3 cells is due to induction of apoptosis, genomic DNA fragmentation was assessed by comet assay. Cells were treated with different doses of SAP (control, 2µg/µL, 4µg/µL and 8µg/µL) for 24 hrs and comet assays were performed as described above. The number of apoptotic cells and tail lengths were assessed under a fluorescence microscope. A dose-dependent increase in the number of apoptotic cells and average tail length of comet was observed in all the three cancer cell lines tested. However, no significant number of control cells was observed undergoing apoptosis. In A549, the tail length of the apoptotic cells treated with 2, 4 and 8 µg/µl of SAP were 139.90±6.02 µm, 217.26 ±6.84µm and 259.57 ±16.27µm [Figure 2(a-d)] respectively.

Similar observations were found in HeLa with tail lengths of 91.60±17.09µm, 176.45 ±12.58 µm and 162.69±3.54µm [Figure 2(e-h)] and in PC3 with tail lengths of 112.83±10.54µm, 225.67 ±19.84µm and 241.64±61.13µm cells treated with 2, 4 or 8µg/µl of SAP respectively [Figure 2 (i-l)]. Independent t-tests of average tail lengths between groups of the three cell lines showed a strong statistically significant difference ($p<0.0001$ at 95% CI) [Figure 2(m)]. The results showed that SAP induces genomic DNA fragmentation in PC3, A549 and HeLa, which is the hallmark of apoptosis, in all the cell lines tested in a dose-dependent manner. The results suggest that SAP induces apoptosis leading to cell death.

SAP induces A549 and HeLa cells apoptosis through caspase-3 activation and PARP deactivation while in PC3 independent of caspase and PARP

To determine the molecular mechanism of the apoptosis induced by SAP, the activation of executioner caspase-3 and deactivation of PARP in A459, PC3 and HeLa cells were assessed by Western blotting. The three cell lines were treated with various doses of SAP for 24 hrs and immunoblotted against caspase-3 or PARP antibodies. The results showed that treatment of SAP to A549 and HeLa cells leads to the cleavage of caspase-3 and PARP proteins. On the other hand, in PC3 cells no cleavage of caspase-3 and PARP proteins was observed [Figure 3]. When assessed the cleavage of caspase-7 and caspase-9, cleavage of none was observed in case of PC3 (result not shown). The results suggest that SAP induces cell apoptosis in a caspase- and PARP-dependent manner in A549 and HeLa cells but in a caspase- and PARP-independent manner in PC3 cells.

SAP induces apoptosis through MAPK pathways

To determine the possible pathways of the apoptosis induced by SAP, activation of MAPK pathways was assessed as it plays important roles in cell survival and death. Cells were treated with different doses of SAP for 24 hrs and immunoblotted against the total as well as phosphorylated p38, ERK, or SAPK/JNK antibodies. The results showed that SAP leads to phosphorylation of p38, ERK, and SAPK/JNK proteins in a dose-dependent manner in A549 and HeLa cells whereas in PC3 cells significant increase in phosphorylation in a dose-dependent manner is observed only in p38 protein. Phosphorylation of SAPK/JNK and ERK proteins in PC3 were observed only in the highest dose of SAP. Therefore, SAPK/JNK and ERK pathway may not be directly involved in the SAP induced apoptosis in PC3 [Figure 4]. To confirm

the involvement of ERK, p38 or SAPK/JNK in apoptosis of HeLa and A549 cells, specific inhibitors for ERK, p38, and SAPK/JNK were used and the results revealed role of p38 in HeLa and ERK in A549 cells [Figure 5] as the pre-treatment of SB203580 and FR180204 could rescue the A549 and HeLa cell death from SAP treatment respectively.

SAP promotes cell cycle arrest at S phase in A549 and HeLa cells.

As seen with anticancer drugs, which arrests cell cycle at specific points and thereby inducing apoptosis by destabilizing the normal biochemical processes of the cell, the anti-cancer activity of SAP on A549, HeLa and PC3 cells would have affected the normal cell cycle. To determine whether the mechanism of action of SAP for inducing apoptosis is due to the arrest of the cell cycle, cell cycle analysis was performed. Cells treated with varying doses of the SAP for 12 hrs were subjected to flow cytometry analysis after staining with PI. An increase in the cell population at the S phase was observed in A549 and HeLa cells treated with SAP. Although independent t-test between control and cells treated with 8µg/µL ($2xIC_{50}$) showed a statistically significant increase in cells at S phase in both HeLa and A549 cells ($p<0.05$), there was no statistically significant change in the population of cells at G0/G1 stage in both the cell lines. Reduction in the cell population at the G2/M phase was also observed in both the cell lines with a statistically significant difference between control and cells treated with 8µg/µL. Contrastingly, cell cycle analysis of PC3 cells treated with SAP showed arrest at the G1 phase in a statistically significant manner between control and treated cells ($p<0.05$), and also a consistent population was seen in S phase [Figure 6]. We also observed a reduction of the number of cells at the G2M phase in a dose-dependent manner with statistical significance compared to untreated cells ($p<0.01$).

Discussion:

Sericin protein is an important bioresource with many biological applications that is underutilized and segregated as waste by silk industries. Earlier studies on sericin from *B. mori* have indicated pharmaceutical and cosmetic applications as well as anti-cancer properties on cancer cell types and mouse models pointing towards use of the protein as nutritional supplements in preventive medicine. Moreover, recent advancement in use of peptides as anti-cancer agents further opens up avenues for use of naturally available peptides for the purpose. With difference in species of the silk moth and diverse feeding habits, the composition and texture of silk fibres are different owing to variation in economic values. Amino acid composition analysis of sericin from *B. mori* and *A. pernyi* revealed that the two sericin have different amino acid composition [13,15–17]. Therefore, amino acid composition of sericin from *Antheraea proylei* J. was analysed and the results revealed that amino acid composition of sericin of *Antheraea proylei* J. is different from that of B. mori and *A. pernyi* [Table 1]. Our findings suggest that sericin protein is highly diverse and may have different bioactivities. Analysis of cell cytotoxicity and anticancer evaluations remains limited to domesticated species of silkworm, *B. mori*. Our finding is the first of its kind report on the anti-cancer property of sericin from *A. proylei* J. cocoons.

Our analysis of sericin from *A. proylei* J. on cell cytotoxicity by microscopy indicated signs of abnormal cell morphology such as detachment, round up structures and signs of membrane blebbing. We further determined the IC_{50} value of SAP on the three cell lines by MTT assay which indicated a dose-dependent response on all the three cell lines with different IC_{50} values [Figure 1(g)]. The difference in IC_{50} values of the three cell lines may be due to difference in susceptibility of sericin as observed in various earlier studies with other agonists [18,19]. Our study is in agreement with earlier findings of sericin from *B. mori* that SAP has anti-proliferative activity [10].

Certain cell death pathways such as autophagy and apoptosis share similar morphological changes [20]. To negate out the possibility of undergoing cell autophagy, expression of autophagy related genes; ATG1, ATG-5, DRAM and LC3 were assessed by semi qPCR after SAP treatments. No change in the expression of the autophagy related genes was observed (data not shown). However, comet assay revealed that SAP significantly induces genomic DNA fragmentation in a dose-dependent manner strongly suggesting induction of cell death through apoptosis [Figure 2].

Further molecular events leading to genomic DNA fragmentation were investigated using Western blot analysis in which a caspase-3 and PARP dependent cell death was observed in A549 and HeLa cells whereas caspase-3 as well as PARP independent mechanism was observed in PC3 cells. The difference on the dependence of caspase-3 and PARP may be due to difference in the genotypes of the cancer cell lines or the type of agonists used. Cancer cells have evaded normal cell death through a plethora of molecular changes and evading caspase dependent cell death is one of the mechanisms observed in many cell lines. The finding in the present studies that SAP induces PC3 apoptosis independent of caspase and PARP is parallel with the findings of previous studies on plant extracts [21–23]. Caspase-3, a member of the caspase family plays a central role in inactivation of PARP by cleavage at DEVD site leading to fragmentation of the chromosome to 50kb fragments [24]. In case of HeLa and A549, our observation of caspase-3 activation and PARP deactivation after subsequent exposure to SAP corroborates the fragmented DNA observed in comet assay. Interestingly, absence of caspase-3 activation and PARP inactivation in PC3 warrants a different mechanism leading to DNA fragmentation and apoptosis needing further analysis of the mechanism.

To investigate the signalling pathways of the apoptosis induced by SAP, MAPK pathways were selected since it plays important roles in cell survival and cell death. The findings in our study indicate that SAP induces apoptosis in A549 and HeLa cells through activation of p38, SAPK/JNK and ERK pathways. Inhibition of p38 rescued cells from apoptosis in HeLa cells whereas inhibition of ERK phosphorylation had similar consequence in A549 cells. The findings indicate role of p38 and ERK in trigger of apoptotic pathway in HeLa and A549 cells induced by SAP [Figure 7]. However, SAP induces cell apoptosis through p38 pathways activation but not SAPK/JNK and ERK pathways and independence of caspase-3 and PARP in the case of PC3. Our observations are in agreement with earlier studies in which p38 and JNK are reported as stress activated and involved in apoptosis of A549 cells [25], HeLa [26] and PC3 cells [27,28] Although the role of ERK in apoptosis remains controversial it is observed that DNA damage can induce ERK phosphorylation and further leading to cell death [29]. Moreover, the role of ERK in cell

death is dependent on cell lineage and intensity as well as duration of pro- or anti-apoptotic signal of ERK1/2. Our observation of high intensity phosphorylation in PC3 cells in the highest dose may be a result of extensive DNA damage activating ERK for its pro-apoptotic signal [30].

Arrest of cell cycle at specific points is a complex molecular mechanism and our observation of blockage of cell cycle progression induced by SAP at G0/G1 in PC3 and S phase in A549 and HeLa reveals an interesting phenomenon suggesting different mechanism of cell cycle arrests for different cell lineages. Further investigation is warranted to explain the molecular mechanisms of different cell cycle arrest induced by SAP.

Conclusion:

The SAP in this study induces apoptosis in lung, cervical, and prostate cancer cell lines as observed in the assessment of cell death and genomic DNA fragmentation with IC_{50} values of 3.4 to 3.9 µg/µl through activation of MAPK pathways. However, A549 and HeLa cells follow a molecular mechanism of caspase- and PARP-dependent while in PC3 it is a caspase- and PARP-independent mechanism. Further, SAP induces apoptosis in A549 cells through activation of ERK and in PC3 and HeLa cells through p38. The difference in the molecular mechanisms of apoptosis induced by SAP in A549 and HeLa cell lines and in PC3 cell lines may be due to the difference in the genotypes of the cancer cell lines.

The overall results of the present study envisage the possibility of using SAP as an anti-tumorigenic agent. The study is limited to the fact that the target cellular proteins where SAP binds needs to be determined. Further, the study opens up avenues for use of peptides that can act as anti-cancer agents which can increase the specificity and efficacy of drug designs in the future.

Abbreviations:

PARP: Poly (ADP-ribose) polymerase

MAPK: Mitogen-activated protein kinase

JNK: Jun N-terminal kinase

mins: Minutes

hr: Hour

DMSO : Dimethyl sulfoxide

EDTA : Ethylenediaminetetraacetic acid

SDS : Sodium dodecyl sulfate

SAP. : Sericin from *Antheraea proylei* J.

BCA : Bicinchoninic Acid

PAGE : Polyacrylamide gel electrophoresis

PBS : Phosphate-buffered saline

SD : Standard deviation

SAPK/JNK: Stress-activated protein kinases/Jun amino-terminal kinases

ATG1 : AuTophaGy related 1

ATG-5: AuTophaGy related 5

DRAM: DNA Damage Regulated Autophagy Modulator

LC3: Microtubule Associated Protein 1 Light Chain 3 Alpha

Declarations:

Availability of data and materials

All data generated or analysed during this study are included in this published article

Ethics approval and consent to participate

Not applicable

Consent to publish

Not applicable

Funding

Not applicable

Authors' Contributions

PJD and ARS performed experiments. PJD, ARS and LSS analysed the data. PJD and LSS wrote the manuscript. LRS and SKD reviewed the systematic review. All authors read and approved the final manuscript.

Competing interests

The authors declare that the research was conducted in the absence of any commercial or financial relationships that could be construed as a potential conflict of interest.

Acknowledgements

The authors are grateful to the Directorate of Sericulture, Government of Manipur, Manipur, India and Mr. P.Ibohal (Farm Overseer, Uyumpok Tasar Silk Farm) for providing the silkworm cocoons.

References:

1. Bray F, Ferlay J, Soerjomataram I, Siegel RL, Torre LA, Jemal A. Global cancer statistics 2018: GLOBOCAN estimates of incidence and mortality worldwide for 36 cancers in 185 countries. CA Cancer J Clin. Wiley Online Library; 2018;68:394–424.
2. Weiderpass E. Lifestyle and cancer risk. J Prev Med Public Heal. 2010;
3. Katzke VA, Kaaks R, Kühn T. Lifestyle and cancer risk. Cancer J. (United States). 2015.
4. Yun H, Oh H, Kim MK, Kwak HW, Lee JY, Um IC, et al. Extraction conditions of Antheraea mylitta sericin with high yields and minimum molecular weight degradation. Int J Biol Macromol. Elsevier; 2013;52:59–65.
5. Kunz RI, Brancalhão RMC, Ribeiro L de FC, Natali MRM. Silkworm sericin: properties and biomedical applications. Biomed Res Int. Hindawi; 2016;2016.
6. Sasaki M, Kato N, Watanabe H, Yamada H. Silk protein, sericin, suppresses colon carcinogenesis induced by 1, 2-dimethylhydrazine in mice. Oncol Rep. Spandidos Publications; 2000;7:1049–101.
7. Zhaorigetu S, Sasaki M, Kato N. Consumption of sericin suppresses colon oxidative stress and aberrant crypt foci in 1,2-dimethylhydrazine-treated rats by colon undigested sericin. J Nutr Sci Vitaminol (Tokyo). 2007;
8. Zhaorigetu S, Sasaki M, Watanabe H, KATo N. Supplemental silk protein, sericin, suppresses colon tumorigenesis in 1, 2-dimethylhydrazine-treated mice by reducing oxidative stress and cell proliferation. Biosci Biotechnol Biochem. Taylor & Francis; 2001;65:2181–6.
9. Zhaorigetu S, Yanaka N, Sasaki M, Watanabe H, Kato N. Silk protein, sericin, suppresses DMBA-TPA-induced mouse skin tumorigenesis by reducing oxidative stress, inflammatory responses and endogenous tumor promoter TNF-$α$. Oncol Rep. Spandidos Publications; 2003;10:537–43.
10. Kaewkorn W, Limpeanchob N, Tiyaboonchai W, Pongcharoen S, Sutheerawattananonda M. Effects of silk sericin on the proliferation and apoptosis of colon cancer cells. Biol Res. Sociedad de Biología de Chile; 2012;45:45–50.
11. Kumar JP, Mandal BB. Silk sericin induced pro-oxidative stress leads to apoptosis in human cancer cells. Food Chem Toxicol. Elsevier; 2019;123:275–87.
12. Zhang WM, Lai ZS, He MR, Xu G, Huang W, Zhou DY. Effects of the antibacterial peptide cecropins from Chinese oak silkworm, Antheraea pernyi on 1, 2-dimethylhydrazine-induced colon carcinogenesis in rats. Di 1 jun yi da xue xue bao= Acad J first Med Coll PLA. 2003;23:1066–8.
13. Silva SS, Kundu B, Lu S, Reis RL, Kundu SC. Chinese oak tasar silkworm antheraea pernyi silk proteins: Current strategies and future perspectives for biomedical applications. Macromol Biosci.

Wiley Online Library; 2019;19:1800252.

14. Olive PL, Banáth JP. The comet assay: A method to measure DNA damage in individual cells. Nat Protoc. 2006;
15. Yang M, Zhou G, Shuai Y, Wang J, Zhu L, Mao C. Ca 2+-induced self-assembly of Bombyx mori silk sericin into a nanofibrous network-like protein matrix for directing controlled nucleation of hydroxylapatite nano-needles. J Mater Chem B. Royal Society of Chemistry; 2015;3:2455–62.
16. Yang M, Shuai Y, Zhang C, Chen Y, Zhu L, Mao C, et al. Biomimetic nucleation of hydroxyapatite crystals mediated by Antheraea pernyi silk sericin promotes osteogenic differentiation of human bone marrow derived mesenchymal stem cells. Biomacromolecules. ACS Publications; 2014;15:1185–93.
17. Malay AD, Sato R, Yazawa K, Watanabe H, Ifuku N, Masunaga H, et al. Relationships between physical properties and sequence in silkworm silks. Sci Rep. Nature Publishing Group; 2016;6:27573.
18. Kabir MF, Mohd Ali J, Abolmaesoomi M, Hashim OH. Melicope ptelefolia leaf extracts exhibit antioxidant activity and exert anti-proliferative effect with apoptosis induction on four different cancer cell lines. BMC Complement Altern Med [Internet]. BioMed Central Ltd.; 2017 [cited 2020 Dec 2];17:252. Available from: http://bmccomplementalternmed.biomedcentral.com/articles/10.1186/s12906-017-1761-9
19. Denel-Bobrowska M, Lukawska M, Oszczapowicz I, Marczak A. M Denel-Bobrowska1 et al [Internet]. Asian Pacific J. Cancer Prev. West Asia Organization for Cancer Prevention (WAOCP); 2016 Sep. Available from: http://journal.waocp.org/article_38738.html
20. Cooper KF. Till death do us part: the marriage of autophagy and apoptosis. Oxid Med Cell Longev. Hindawi; 2018;2018.
21. DebRoy S, Kramarenko II, Ghose S, Oleinik N V, Krupenko SA, Krupenko NI. A novel tumor suppressor function of glycine N-methyltransferase is independent of its catalytic activity but requires nuclear localization. PLoS One. Public Library of Science; 2013;8:e70062.
22. Reddivari L, Vanamala J, Chintharlapalli S, Safe SH, Miller Jr JC. Anthocyanin fraction from potato extracts is cytotoxic to prostate cancer cells through activation of caspase-dependent and caspase-independent pathways. Carcinogenesis. Oxford University Press; 2007;28:2227–35.
23. Zhang M, Liu H, Tian Z, Griffith BN, Ji M, Li QQ. Gossypol induces apoptosis in human PC-3 prostate cancer cells by modulating caspase-dependent and caspase-independent cell death pathways. Life Sci. Elsevier; 2007;80:767–74.
24. Boulares AH, Yakovlev AG, Ivanova V, Stoica BA, Wang G, Iyer S, et al. Role of Poly(ADP-ribose) Polymerase (PARP) Cleavage in Apoptosis CASPASE 3-RESISTANT PARP MUTANT INCREASES RATES OF APOPTOSIS IN TRANSFECTED CELLS* [Internet]. 1999. Available from: http://www.jbc.org/
25. Taylor CA, Zheng Q, Liu Z, Thompson JE. Role of p38 and JNK MAPK signaling pathways and tumor suppressor p53 on induction of apoptosis in response to Ad-eIF5A1 in A549 lung cancer cells. Mol Cancer. 2013;

26. Zhang L, Yang X, Li X, Li C, Zhao L, Zhou Y, et al. Butein sensitizes HeLa cells to cisplatin through the AKT and ERK/p38 MAPK pathways by targeting FoxO3a. Int J Mol Med. Spandidos Publications; 2015;36:957–66.
27. Hilchie AL, Furlong SJ, Sutton K, Richardson A, Robichaud MRJ, Giacomantonio CA, et al. Curcumin-induced apoptosis in PC3 prostate carcinoma cells is caspase-independent and involves cellular ceramide accumulation and damage to mitochondria. Nutr Cancer. Taylor & Francis; 2010;62:379–89.
28. Rodríguez-Berriguete G, Fraile B, Martínez-Onsurbe P, Olmedilla G, Paniagua R, Royuela M. MAP kinases and prostate cancer. J Signal Transduct. Hindawi; 2012;2012.
29. Mebratu Y, Tesfaigzi Y. How ERK1/2 activation controls cell proliferation and cell death: Is subcellular localization the answer? Cell cycle. Taylor & Francis; 2009;8:1168–75.
30. Tang D, Wu D, Hirao A, Lahti JM, Liu L, Mazza B, et al. ERK activation mediates cell cycle arrest and apoptosis after DNA damage independently of p53. J Biol Chem. 2002;

Figures

Figure 1

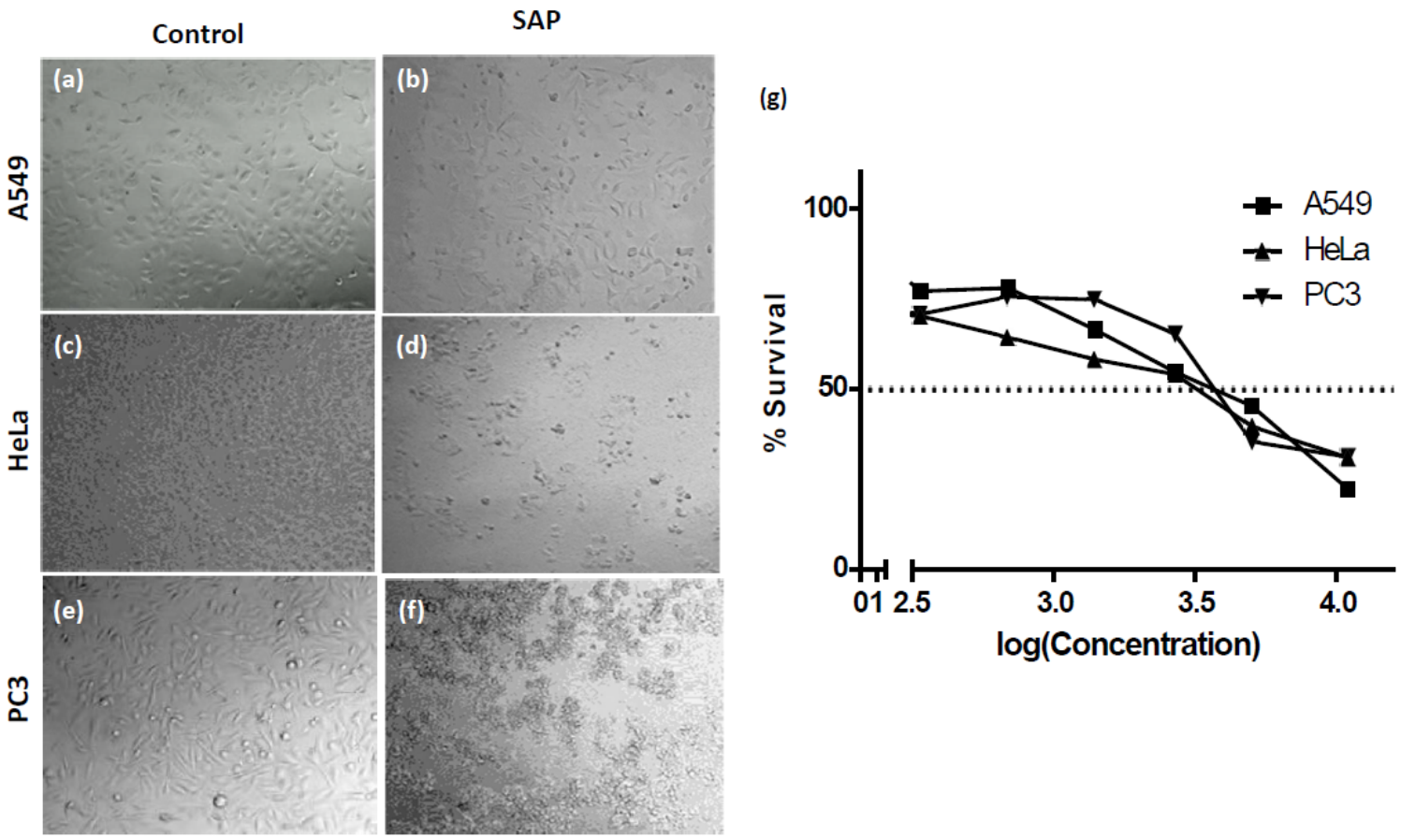

Figure 1

SAP induces cytotoxicity in A549, HeLa, and PC3 cells: Morphological changes were observed under a simple microscope and acquired pictures; (a-b) A549, (c-d) HeLa, and (e-f) PC3 cells. (g) survival curves for inhibition of cell proliferation after treatment with different doses of SAP were analyzed by MTT assay and IC50 values were determined.

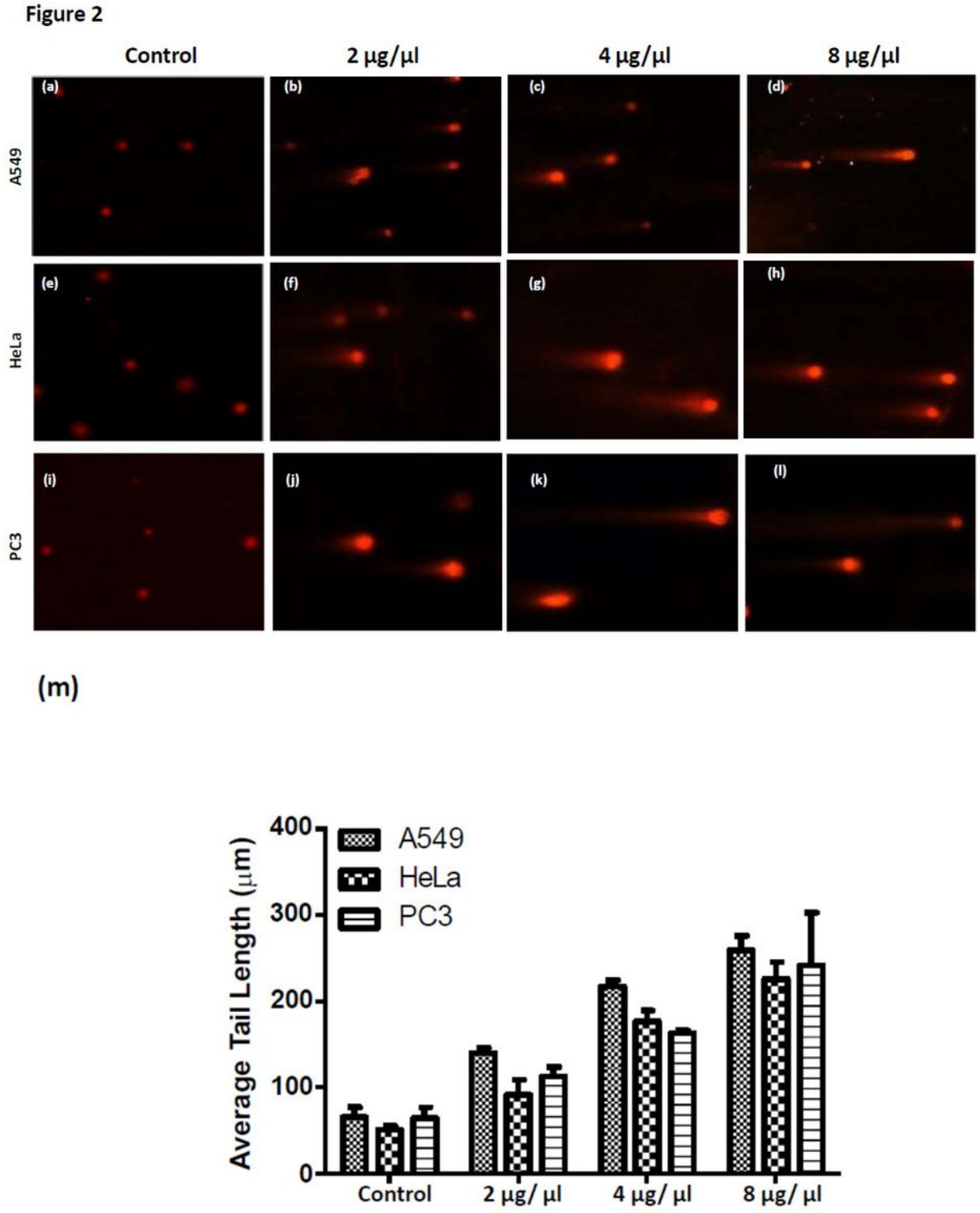

Figure 2

SAP induces genotoxicity: (a-l) gDNA fragmentation was assessed by comet assay after SAP treatment to A549 (a-d), HeLa (e-h), and PC3 (i-l) for 24 h. Negative controls were treated with PBS (a, e, and i) and different doses of SAP; 2µg/µl (b,f, and i), 4µg/µl (c, g and k) and 8µg/µl (d, h and l). Pictures were captured under an inverted fluorescence microscope. (m) the average tail lengths of the 50 apoptotic cells each were measured and the graph between the dose of SAP and the average tail lengths of each cell line is shown. Comparison of average tail length within groups of each cell lines showed strong statistical significance ($p<0.0001$).

Figure 3

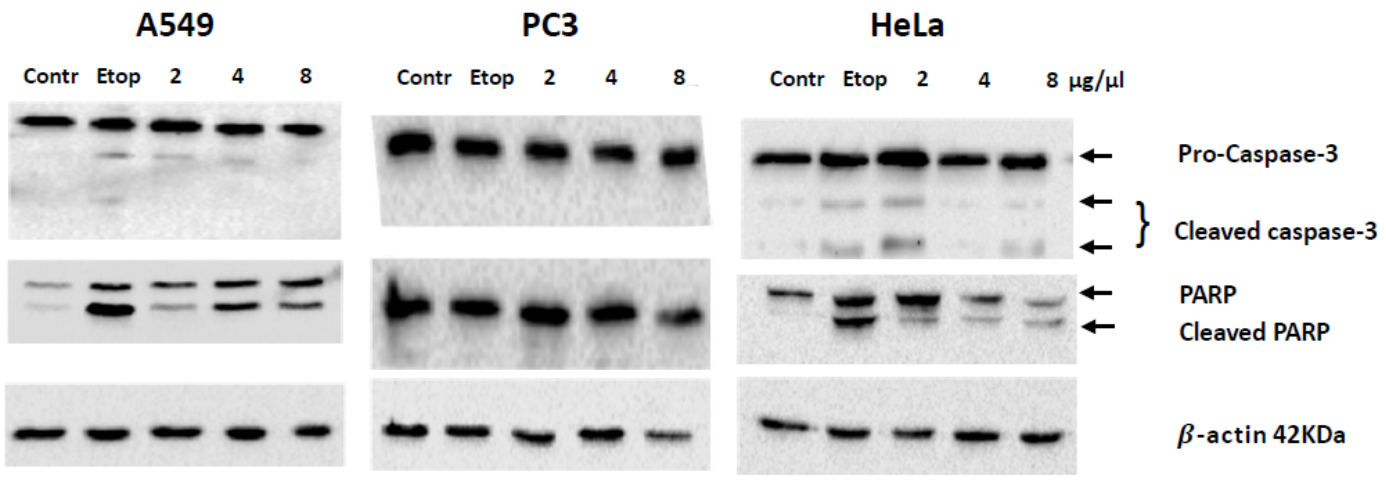

Figure 3

SAP induces cleavage of caspase-3 and PARP proteins in A549 and HeLa cells but not in PC3 cells. Cells were treated with PBS (Contr) as the negative control, Etoposide (59.2µmol) (Etop) as positive control and different doses of SAP (2,4, and 8 µg/µl final concentration) for 24 hrs. Western blots were performed against anti-pro-caspase-3, anti-cleaved caspase-3, anti-PARP, and anti-cleaved PARP antibodies. Western blot against anti-β -actin antibody was also performed on the same respective membranes to normalize the proteins loaded.

Figure 4

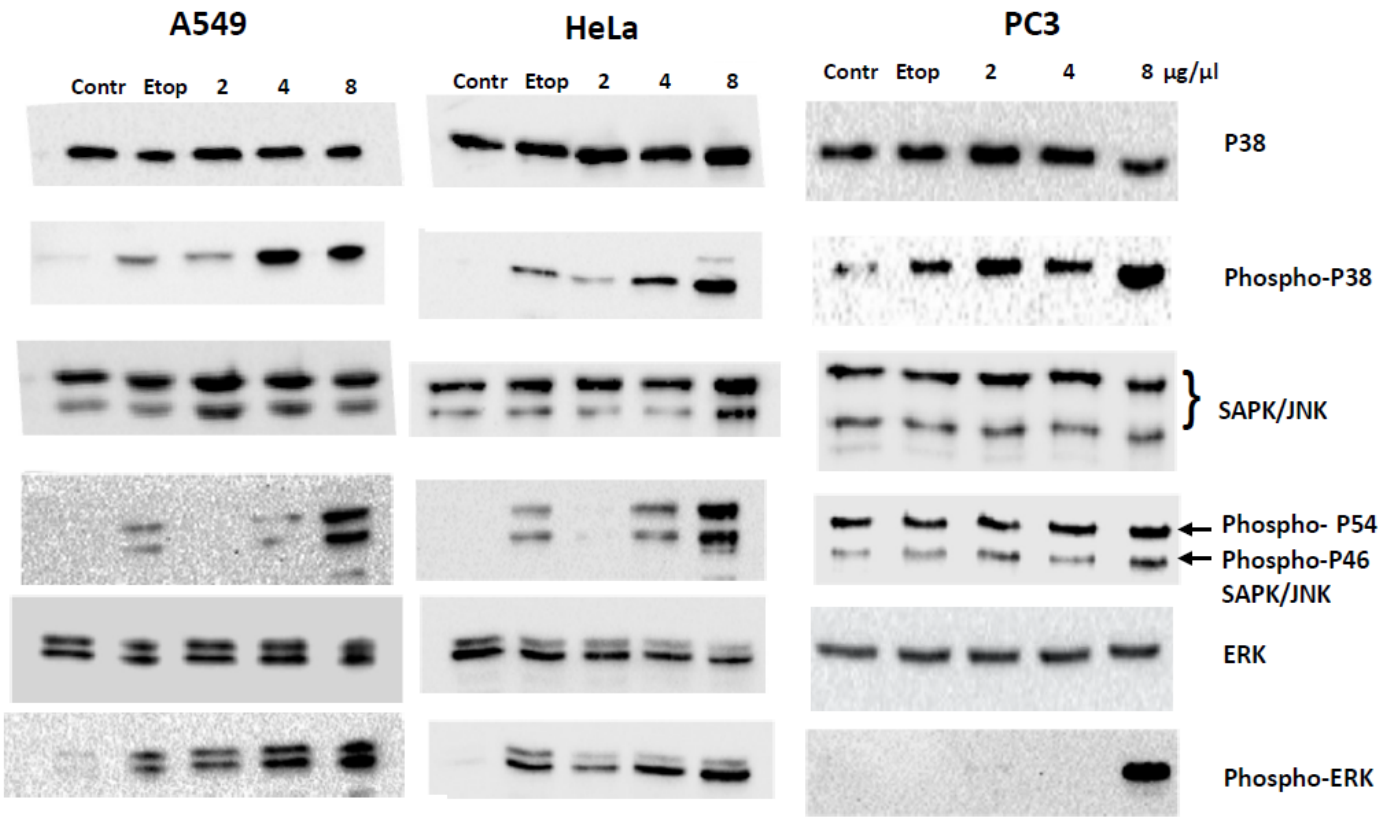

Figure 4

SAP induces MAPK pathways: Cells were treated with PBS (Contr) as the negative control, Etoposide (59.2µmol) (Etop) as the positive control, and different doses of SAP (2,4, and 8 µg/µl final concentration) for 24 hrs. Western blots were performed against anti-p38, anti-phospho-p38, anti-SAPK/JNK, anti-phospho-SAPK/JNK, anti-ERK, and anti-phospho-ERK.

Figure 5

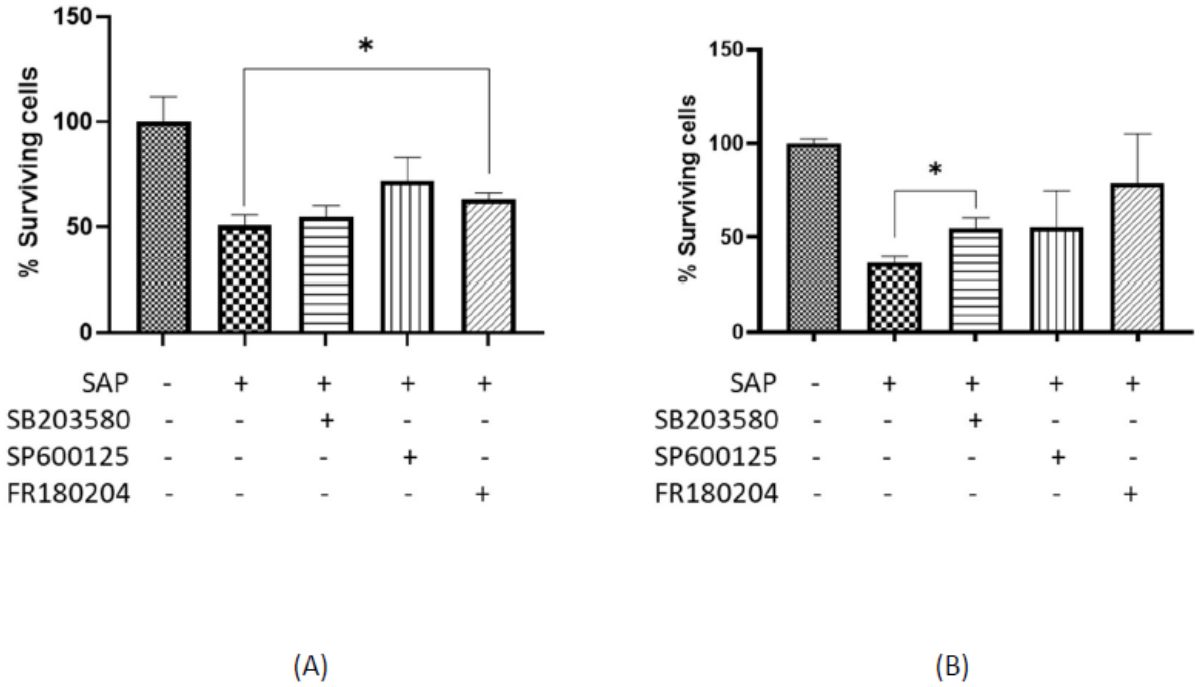

Figure 5

SAP induces apoptosis in A549 cells through phosphorylation of ERK (A) and through phosphorylation of p38 in HeLa cells (B): Cells treated with SAP alone or with inhibitors of p38 (SB3580) or JNK (SP600125) or ERK (FR180204) were incubated for 24 hrs and quantified with MTT assay. Statistically significant recovery of cells from apoptosis were determined by comparison with cells treated with SAP alone and with specific inhibitors as indicated (* indicates $p<0.005$)

Figure 6

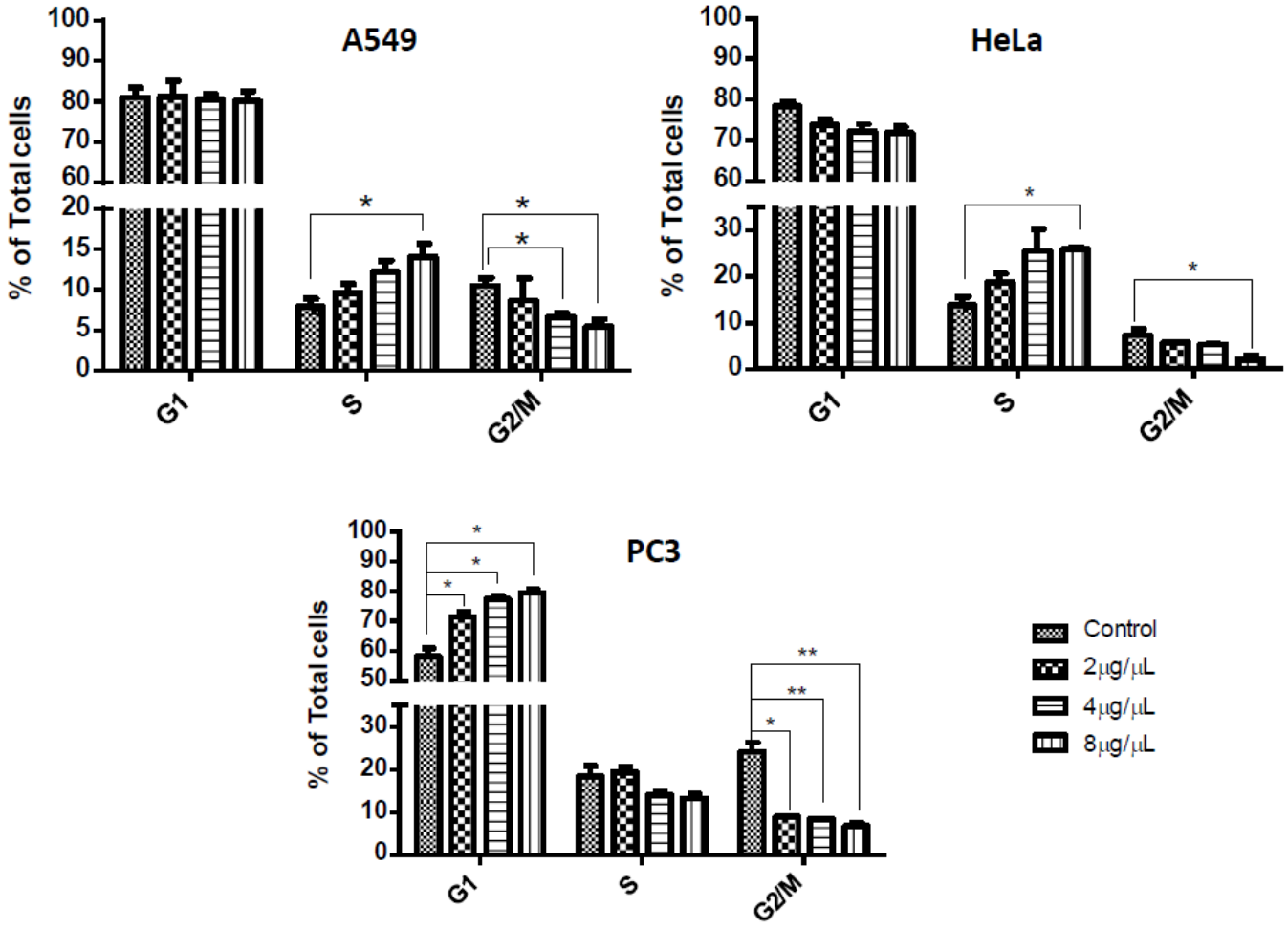

Figure 6

SAP induces cell cycle arrest: Cells were treated with PBS (Contr) as the negative control and different doses of SAP (2,4, and 8 μg/μl final concentration) for 24 hrs. Cell cycles were analyzed by flow cytometry. The percentages (%) of total cells at each phase, G1, S, or G2M are indicated against each cell line. (* indicates $p<0.05$, ** indicates $p<0.01$)

Figure 7

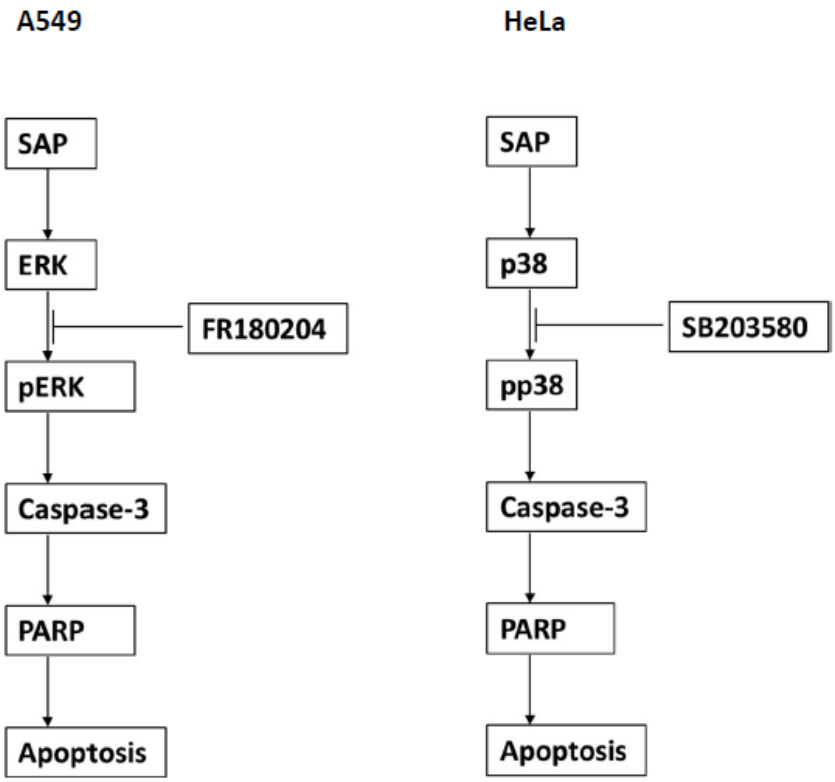

Figure 7

Schematic presentation of molecular pathways of apoptosis induced by SAP: A549 and HeLa cells treated with inhibitor of ERK and p38 phosphorylation respectively could rescue the cells from apoptosis induced by SAP indicating different mechanisms of cell death in different cell lines.

Supplementary Files

This is a list of supplementary files associated with this preprint. Click to download.

- uncroppedimages.pdf